

RESIDUAL DISTRIBUTION SCHEMES FOR THE COMPUTATION OF HYPERSONIC FLOWS WITH STRONG BOW SHOCK WAVES: ENFORCING TOTAL ENTHALPY CONSERVATION

Jesus Garicano^{1,2,*}, Andrea Lani¹, Herman Deconinck^{1,2} and Gérard Degrez^{1,2}

¹ von Karman Institute for Fluid Dynamics,
Waterloose Steenweg, 72, Sint-Genesius-Rode, 1640, België
² Service Aéro-Thermo-Mécanique, Université Libre de Bruxelles,
Avenue F. D. Roosevelt, 50, Bruxelles, 1050, Belgique

* Corresponding author: Jesus Garicano Mena, jesus.garicano.mena@vki.ac.be

Key words: Residual Distribution, Flux Difference Splitting, Heat Flux, Hypersonic Flow.

Abstract. In this contribution we retrieve from the literature a known (but so far relatively unexplored) parallelism existing between *Residual Distribution* and *stabilized Finite Elements*. We use that relation as a basis to derive two new *Residual Distribution* schemes with better properties regarding the preservation of the upstream total enthalpy level. These schemes are employed for the simulation of inviscid hypersonic flow fields, producing better results than the reference schemes. Finally, these schemes are applied to predict the heat flux induced by an hypersonic viscous flow around a blunt body.

1 INTRODUCTION

Numerical simulation of hypersonic flows is a challenging activity, since the complexity characterizing compressible flow aerodynamics have to be addressed together with additional high-temperature effects phenomena (see Reference¹).

Residual Distribution (RD^1) Methods evince several advantageous features for the computation of compressible flows. Among them, we stress the following:

- A maximum principle (Local Extrema Diminishing) borrowed from Finite Volume (FV), which allows to capture discontinuities monotonically on general unstructured grids;
- Being based on finite element (FE) approximation theory, it is possible to obtain, on a compact stencil, second-order order accurate solutions on unstructured grids;

¹ RD methods are also known under the name of Fluctuation Splitting (FS) schemes.

- Less grid sensitivity on simplicial meshes, thanks to a built-in multidimensional dissipation property.

These reasons make *RD* schemes appealing for the simulation of atmospheric entry flow problems. In a recent study (cfr. Ref²), the flow field and heat flux prediction capabilities of *RD* methods applied to the computation of high temperature flow fields have been investigated: *RD* methods are capable of producing accurate flow solutions and heat flux prediction for flows where no shock waves are present, irrespective of whether the gas is modeled as ideal and inert or in non-equilibrium; for both 2D and axisymmetric computations. Unfortunately, straightforward application of the same *RD* technique to flows including strong curved shocks yields incorrect heat flux predictions. Consider the $Ma = 17.5$ flow around a cylinder: the hottest spot in the flow field is located, surprisingly, away from the stagnation line -Fig. 1(a)- and consequently the heat flux cannot be correct, Fig. 1(b). As established in reference², the way *RD* multi-dimensional upwind schemes capture the shock wave, and in particular how total enthalpy is handled across the shock, seems to be the responsible for this unexpected result.

Our priority is thus the derivation of shock capturing *RD* schemes that recover the upstream total enthalpy level in the downstream side of a strong bow shock. The obvious way to achieve this objective is simply to set the temperature of every degree of freedom to the value:

$$T = T_{t,\infty} = T_\infty + \frac{1}{2c_p} (\|\vec{u}_\infty\|^2 - \|\vec{u}\|^2). \quad (1)$$

This approach is effective in maintaining total enthalpy uniform away from the shock wave. Nevertheless, this naive strategy is strictly valid only for inviscid flows where the fluid comes from a region with uniform properties; even worse, it can induce problems in convergence to steady state and it is not generally applicable.

Therefore we seek for alternative techniques to obtain post-shock total enthalpy recovery. The equations describing the problem of our interest are introduced in the next section, together with a general overview of *RD* methods. The third section recovers a known analogy between *RD* and stabilized *FE* methods, which we employ to improve the shock capturing properties of *RD* schemes. The performance of the new technique derived is evaluated for both inviscid and viscous hypersonic flow configurations. Our findings are summarized in the closing section of this contribution.

2 RESIDUAL DISTRIBUTION FOR THE NAVIER-STOKES EQUATIONS

The Navier-Stokes equations describe the conservation of mass, momentum and energy of a flow field. In compact, vector form they read:

$$\frac{\partial \vec{U}}{\partial t} + \nabla \cdot \vec{F}^c = \nabla \cdot \vec{F}^d + \vec{S}, \quad (2)$$

where \vec{U} stands for the vector of conserved variables. For an inert, ideal gas \vec{U} includes the density ρ , the momentum ρu_j and the total energy ρE .

Tensors \vec{F}^c and \vec{F}^d describe the convective and diffusive fluxes of the conserved quantities. For the simplified thermodynamical model employed in this work vector \vec{S} is identically zero; it would be non-zero if a gas flow out of chemical and/or thermal equilibrium (reference¹) was to be simulated.

The components of the convective flux tensor are given by:

$$\vec{F}_j^c = [\rho u_j, \quad \rho u_i u_j + p \delta_{i,j}, \quad \rho H u_j]^t, \quad (3)$$

whereas the diffusive flux tensor is:

$$\vec{F}_j^d = [0, \quad \tau_{i,j}, \quad \tau_{i,j} u_j - q_i]^t. \quad (4)$$

We describe briefly the *RD* discretization for the System of Equations 2, as condensed from references³⁻⁵. The solution sought is expressed by means of a finite element representation on P1 linear simplices.

$$\vec{U}^h(\vec{x}, t) = \sum_{j=1}^{\#DOF} \vec{U}_j(t) N_j(\vec{x}), \quad \text{where } N_j(\vec{x}_k) = \delta_{jk}. \quad (5)$$

The steady state residual for element Ω gathers contributions from the convective and dissipative terms:

$$\vec{\Phi}^\Omega = \int_\Omega \left(\frac{\partial \vec{F}_j^c}{\partial x_j} - \frac{\partial \vec{F}_j^d}{\partial x_j} \right) dv = \vec{\Phi}^{c,\Omega} - \vec{\Phi}^{d,\Omega}. \quad (6)$$

The nodal system of equations is obtained by distributing fractions of the cell residuals $\vec{\Phi}^\Omega$ to the nodes forming part of the cell:

$$\vec{\Phi}_l = \sum_{\Omega_i \in \Xi_l} \vec{\Phi}_l^{\Omega_i}, \quad (7)$$

The convective contribution to the nodal equation of the cell residual is expressed generically as:

$$\vec{\Phi}_l^c = \sum_{\Omega_i \in \Xi_l} B_l^{\Omega_i} (K^\pm) \cdot \vec{\Phi}^{c,\Omega_i} \quad (8)$$

in terms of the so called distribution matrices $B_l^{\Omega_i}$, which depend in turn on the nodal upwind parameters:

$$K_j = \frac{1}{n_D} (A_{j,x} n_{j,x} + A_{j,y} n_{j,y} + A_{j,z} n_{j,z}), \quad (9)$$

where A_{j,x_d} is the Jacobian of the advective flux along direction x_d , n_{j,x_d} are the components of the vectors normal to the element faces and n_D is the dimensionality of the problem.

Different forms of the $B_l^{\Omega_i}$ matrices define different schemes. The most employed second-order accurate linear scheme is the low diffusion A (LDA), defined as:

$$B_l^{\Omega_i, LDA} = (K_l)^+ \cdot \left(\sum_j (K_j)^+ \right)^{-1}. \quad (10)$$

The LDA scheme performs very well for the simulation of smooth flows, as reported in references^{2,3,6}.

For the simulation of shocked flow configurations, the linear, quasi-monotone N scheme is available, given by:

$$\vec{\Phi}_l^{c, \Omega_i, N} = K_l^+ \cdot \left(\vec{U}_l - \vec{U}_{inlet}^{\Omega_i} \right). \quad (11)$$

The *inlet* state $\vec{U}_{inlet}^{\Omega_i}$ reads:

$$\vec{U}_{inlet}^{\Omega_i} = \sum_{l=1} (K_l^-)^{-1} \cdot \sum_{l=1} K_l^- \cdot \vec{U}_l. \quad (12)$$

Please, notice that this scheme is only 1^{st} order accurate and that a $B_l^{\Omega_i}$ matrix cannot be defined for this case

If one is interested in second-order accurate simulation of shocked flows a non-linear scheme is required. Non-linearity is achieved by blending the LDA and the N schemes via a solution dependent function Θ :

$$\vec{\Phi}_l^{c, \Omega_i, B} = \Theta^{\Omega_i} \vec{\Phi}_l^{c, \Omega_i, N} + (I - \Theta) \vec{\Phi}_l^{c, \Omega_i, LDA}, \quad (13)$$

Different choices of Θ^{Ω_i} result in different variants of the blended scheme. The two most common are:

- The original B scheme⁵, where Θ^{Ω_i} is a diagonal matrix whose entries are defined by the ratios of the components of the characteristic decomposition of the nodal residual over the cell residual:

$$\Theta^{\Omega_i} = \text{diag}(\theta_k), \quad \text{with } \theta_k = \frac{\vec{l}_k \cdot \vec{\Phi}_l^{c, \Omega_i}}{\vec{l}_k \cdot \sum_l \vec{\Phi}_l^{c, \Omega_i}} \quad (14)$$

and where \vec{l}_k is the k^{th} left eigenvector.

- The Bx scheme⁷, where Θ^{Ω_i} is the identity matrix times a scalar shock sensor θ , based on a field variable (*i.e.* pressure, temperature or density):

$$\Theta^{\Omega_i} = \theta^{\Omega_i} I. \quad (15)$$

Distribution of diffusive contributions to the cell residual is performed, when a $P1$ element mesh is used, by Galerkin discretization:

$$\vec{\Phi}_j^{d,\Omega} = \int_{\Omega} N_j \nabla \cdot \vec{F}^v dv. \quad (16)$$

From the distribution process introduced before results a system of differential equations controlling the time evolution of the solution at the grid nodes. For l -th node, it reads:

$$\Xi_l \frac{d\vec{U}_l}{dt} + \vec{\Phi}_l^c - \vec{\Phi}_l^d = \vec{0}, \quad (17)$$

where Ξ_l stands for the volume of the median dual cell around l -th node.

The discretization of Eq. 17 is accomplished by means of the *COOLFluiD* solver⁸. Eq. 17 is marched in pseudo-time until a steady state solution is reached, by using an implicit backward Euler integrator. The linear system of equations obtained at each *pseudo-time* step is then solved by one of the Krylov subspace methods provided by the *PETSc* solver library⁹.

Concerning boundary conditions, isothermal wall and supersonic inlet boundary conditions are enforced strongly, whereas far-field, subsonic outlet and inviscid wall boundary conditions are weakly imposed, as detailed in reference³.

3 NUMERICAL CONSERVATION OF TOTAL ENTHALPY ACROSS SHOCK WAVES

Previous results² have lead us to investigate several alternative strategies to modify the numerical dissipation locally across a shock wave. Some of them start from the relationship between *LDA* and *N* schemes reported in⁴:

$$\vec{\Phi}_l^{c,\Omega_i,Nc} = \vec{\Phi}_l^{c,\Omega_i,LDAc} + \vec{\delta}_l^{Diss,Nc}, \quad (18)$$

where $\vec{\delta}_l^{Diss,Nc}$ is the crosswind dissipation that added to the *LDAc* scheme gives back the *Nc* scheme. Eq. 18 substituted into the definition of *B* scheme (Eq. 13) yields:

$$\vec{\Phi}_l^{c,\Omega_i,B} = \vec{\Phi}_l^{c,\Omega_i,LDAc} + \Theta^{\Omega_i} \vec{\delta}_l^{Diss,Nc} = B_l^{\Omega_i,LDAc} \cdot \vec{\Phi}_l^{c,\Omega_i} + \Theta^{\Omega_i} \vec{\delta}_l^{Diss,Nc} \quad (19)$$

Notice this expression is conceptually very close to *stabilized* finite element schemes^{10,11}: first term takes care of advection of smooth information while the second term, locally active (*i.e.* modulated by a shock detector), contributes with additional dissipation to handle strong gradients. Actually, *SUPG* scheme can be expressed into the *RD* formalism through a distribution matrix (derived in reference³):

$$B_l^{\Omega_i, SUPG} = \frac{1}{n_D + 1} I + K_l \cdot \tau, \quad (20)$$

where τ is a matrix of time scales. This τ matrix can be defined in several ways (*cfr.* references^{10,12}); we stick to the definition provided in reference¹³ :

$$\tau = \left(\sum_j |K_j| \right)^{-1}. \quad (21)$$

With the inclusion of the shock capturing term, the *SUPG* scheme in *RD* formalism looks like:

$$\vec{\Phi}_l^{c, \Omega_i, SUPG+SC} = B_l^{\Omega_i, SUPG} \cdot \vec{\Phi}^{c, \Omega_i} + \underbrace{\int_{\Omega_i} \Gamma_{SC} \nabla N_l \nabla \vec{U} \, dv}_{SC_l}. \quad (22)$$

Thanks to the similarity between expressions in Eq. 19 and 22, we can import techniques derived for the *SUPG* methods into the *RD* framework. A *SUPG* shock capturing term capable of recovering the right pre-shock total enthalpy level² has been derived in reference¹⁵ ; and its expression is:

$$S_l^H = \int_{\Omega_i} \Gamma_{SC} \nabla N_l \frac{\partial \vec{U}^H}{\partial \vec{U}} \nabla \vec{U} \, dv, \quad (23)$$

where \vec{U}^H is the vector $[\rho, \quad \rho u_j, \quad \rho H]^t$.

This is precisely what we are looking for. We will test these two new *RD* schemes:

$$\vec{\Phi}_l^{c, \Omega_i, LDA+H-SC} = B_l^{\Omega_i, LDA} \cdot \vec{\Phi}^{c, \Omega_i} + S_{\Omega_i} \Theta^{\Omega_i} \nabla^h N_l \frac{\partial \vec{U}^H}{\partial \vec{U}} \nabla^h \vec{U}, \quad (24)$$

$$\vec{\Phi}_l^{c, \Omega_i, SUPG+H-SC} = B_l^{\Omega_i, SUPG} \cdot \vec{\Phi}^{c, \Omega_i} + S_{\Omega_i} \Theta^{\Omega_i} \nabla^h N_l \frac{\partial \vec{U}^H}{\partial \vec{U}} \nabla^h \vec{U}, \quad (25)$$

where the *constant-per-element* gradients characteristic of *P1* elements are indicated by superscript *h*.

There is, nevertheless, a conceptual difference to bear in mind: matrix Θ does not have residual character while scalar term Γ_{SC} has. The modification to provide Θ^{Ω_i} with residual character is straightforward, but this point does not prevent the method to work correctly (as we will show immediately after); hence this modification is left for future work.

² The possibility of substituting the shock capturing term in the *BCx* by a *FV* flux function formulated in the median dual cell exists as well. In particular, schemes *AUSM+–up2* and *LDFSS2001–2* described in reference¹⁴ could have been used. We have preferred not to do so, because *FV* flux functions are very sensitive to the misalignment between numerical shock waves and the simplicial meshes we employ.

3.1 Effect of the H-SC capturing term for hypersonic inviscid flows

In order to test the combination of the new shock capturing term, we have simulated the $Ma_\infty = 9$ hypersonic flow around a $1m$ in diameter cylinder, described in.¹⁵ The computations shown are performed on a mesh with 121×161 nodes uniformly distributed in the radial and the tangential directions respectively. Energy residuals converged 12 orders of magnitude for all the simulations shown.

Figures 3 and 4 show the quantity $\left(1 - \frac{H_t}{H_{t,\infty}}\right)$ along cuts at $y = 0$ (stagnation line) and $y = 0.25m$ respectively, as predicted by the *BCx* scheme, the *LDA + SC* and the *SUPG + SC* schemes (these last two using the standard shock capture term) and the *LDA + H - SC* and the *SUPG + H - SC* schemes (the same, but with the improved shock capturing term). Fig. 2 plots again $\left(1 - \frac{H_t}{H_{t,\infty}}\right)$ over the whole domain, for the *BCx*, the *LDA + SC* and the *LDA + H - SC* schemes. At the sight of this figures, we conclude that:

- Solutions employing a shock capturing term predict broader numerical shock waves than the *BCx* scheme.
- Shock waves captured with *H - SC* variants of a given scheme are consistently thinner than those obtained with the corresponding standard *SC*.
- *H - SC* schemes are closer to obtain correct post-shock enthalpy level that the other schemes., though
- None of the schemes tested achieves enthalpy-preservation at the stagnation point.

We conclude that schemes with the *H - SC* term should be favored, and possibly complemented with a special treatment of the stagnation point.

3.2 Effect of the H-SC capturing term for hypersonic viscous flows

In this section we study how the newly derived *H - SC* schemes perform when applied to viscous, hypersonic flow fields. We are specially interested on its effect on the predicted heat flux at the stagnation point. To do so we simulate the hypersonic, $Ma_\infty = 8.1$, $Re_\phi = 2.610^5$ flow around a cylinder $40mm$ in diameter, whose wall is assumed to be isothermal at $T_w = 300K$. The upstream pressure and temperature are $p_\infty = 370.7Pa$, $T_\infty = 63.73K$.

A *RD* solution for this problem, obtained with *B* scheme and an additional *carbuncle* fix term, is described in reference⁵ : the right level of the stagnation heat flux was not matched, an overshoot similar to the one shown in Fig. 1(b) was obtained.

Figures 5 and 6 show the dimensionality pressure and the heating at the wall as provided by the *LDA + H - SC* and the *SUPG + H - SC* schemes. These solutions were computed

on a mesh with 161×61 nodes in the radial and the tangential direction respectively ³. and compared with the *FV* solutions in reference¹⁴. Pressure is non-dimensionalized with the Pitot pressure ($p_{10} = 31472.43 Pa$) and heat flux with the value $q_{FR} = 17.5W/cm^2$, given by the Fay-Rydell relation.

Both schemes match reasonably the pressure reference level, with an error lower than 5% in both cases. *LDA + H - SC* schemes predicts a heat flux profile which oscillates around the stagnation point while *SUPG + H - SC* matches very accurately the reference solution. Regarding the oscillatory behavior for the *LDA + H - SC* heat flux, we believe it is consequence of two factors: the very low dissipation of the *LDA* contribution and the regular grid employed. Since the triangular mesh employed is obtained by splitting the quadrilaterals of a structured grid, there is a change of the slope of the diagonals across the symmetry line. This might generate a perturbation in the solution that induces a tiny symmetric recirculation, sufficiently small not to be reflected in the pressure but enough to spoil the heat flux prediction⁴. The *SUPG* scheme, more dissipative, would be capable of dissipating away this perturbation, and thus retrieving the correct level for the heat flux.

4 CONCLUSIONS

In this contribution we have adapted a shock capturing technique from the stabilized *FE* methodology to the *RD* formalism, by taking advantage of a known -but relative unexplored- parallelism between both families of methods. The term so imported has allowed us to derive two different *RD* schemes with improved properties when concerning the preservation of total enthalpy across shock waves numerically captured, the *SUPG + H - SC* and the *SUPG + H - SC* schemes.

These two methods surpass the capabilities of the standard methods they derive from, as it has been demonstrated with the simulation of a hypersonic inviscid flow around a blunt body. Though the evident improvement, stagnation point still poses problems to these new methods, which calls for a special treatment.

Finally, these schemes have been applied for the prediction of hypersonic heating at the stagnation point. Both schemes offer good prediction of the wall pressure. *SUPG + H - SC* scheme matches heat flux well, while *LDA + H - SC* scheme misses it: an explanation for this fact, consistent with previous experiences reported in the literature, has been proposed.

³Hence, coarser in the tangential direction than solutions in references,^{5,14} following ¹⁶.

⁴These behavior has been reported as well for *B* scheme, see reference⁵.

REFERENCES

- ¹ J. D. Anderson. *Hypersonic and High Temperature Gas Dynamics*. McGraw Hill, New York, 1989.
- ² J. Garicano Mena, R. Pepe, A. Lani and H. Deconinck. Experimental Characterization of Hypersonic Nozzle Boundary Layers and Free-Stream Noise Levels. Number AIAA 2014-1391, 52nd AIAA Aerospace Sciences Meeting, Washington(DC), January 2014.
- ³ van der Weide, E. *Compressible flow simulation on unstructured grids using multi-dimensional upwind schemes*. PhD thesis, Technische Universitet Delft, 1998.
- ⁴ Ricchiuto, M. *Construction and analysis of compact residual distribution discretizations for conservation laws on unstructured meshes*. PhD thesis, Université Libre de Bruxelles, 2005.
- ⁵ Sermeus, K. *Multi-Dimensional Upwind Discretization and Application to Compressible Flows*. PhD thesis, Université Libre de Bruxelles, 2013.
- ⁶ Villedieu, N. *High order discretisation by residual distribution schemes*. PhD thesis, Université Libre de Bruxelles, 2009.
- ⁷ Dobes, J. *Numerical Algorithms for the Computation of Steady and Unsteady Compressible Flow over Moving Geometries : Application to Fluid-Structure Interaction*. PhD thesis, Université Libre de Bruxelles, 2007.
- ⁸ Lani, A. *An object oriented and high-performance platform for aerothermodynamic simulations*. PhD thesis, Université Libre de Bruxelles, 2008.
- ⁹ Satish Balay, Jed Brown, , Kris Buschelman, Victor Eijkhout, William D. Gropp, Dinesh Kaushik, Matthew G. Knepley, Lois Curfman McInnes, Barry F. Smith, and Hong Zhang. PETSc users manual. Technical Report ANL-95/11 - Revision 3.4, Argonne National Laboratory, 2013.
- ¹⁰ Hughes, T.J.R. and Mallet, M. A new finite element formulation for computational fluid dynamics: III. The generalized streamline operator for multidimensional advective-diffusive systems. *Computer Methods in Applied Mechanics and Engineering*, 58(3):305–328, 1986.
- ¹¹ Hughes, T.J.R. and Mallet, M. A new finite element formulation for computational fluid dynamics: IV. A discontinuity-capturing operator for multidimensional advective-diffusive systems. *Computer Methods in Applied Mechanics and Engineering*, 58(3):329–336, 1986.
- ¹² Carette, J.C. *Adaptive Unstructured Mesh Algorithms and SUPG Finite Element Method for Compressible High Reynolds Number Flows*. PhD thesis, Université Libre de Bruxelles, 1997.
- ¹³ Kirk, B. S., Carey, G. F., Stogner, R. H., Oliver, T.A., and Bauman P. T. Recent Advancements in Fully Implicit Numerical Methods for Hypersonic Reacting Flows. Number AIAA 2013-2559, 21st AIAA Computational Fluid Dynamics Conference, San Diego, CA, June 2013.
- ¹⁴ Kitamura, K., Shima, E. Towards shock-stable and accurate hypersonic heating computations: A new pressure flux for AUSM-family schemes. *Journal of Computational Physics*, 245:62–83, 2013.
- ¹⁵ Kirk, B. S. Adiabatic shock capturing in perfect gas hypersonic flows. *International Journal for Numerical Methods in Fluids*, 64:1041–1062, 2010.
- ¹⁶ A. Lani. Private communication. 2013.
- ¹⁷ Gnoffo, P. A., White, J. A. Computational aerothermodynamic simulation issues on unstructured grids. In *Proceedings of the 37th AIAA Aerospace Science Meeting and Exhibit*, Portland(OR), 2004. AIAA.

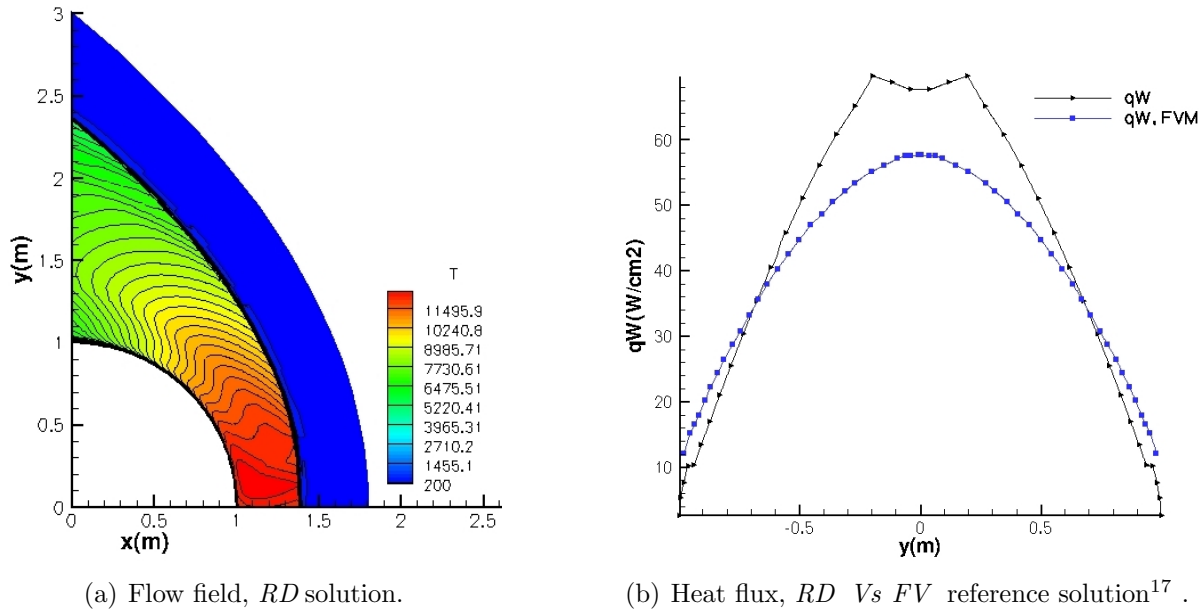


Figure 1: Viscous, hypersonic flow around cylinder, shock wave captured.

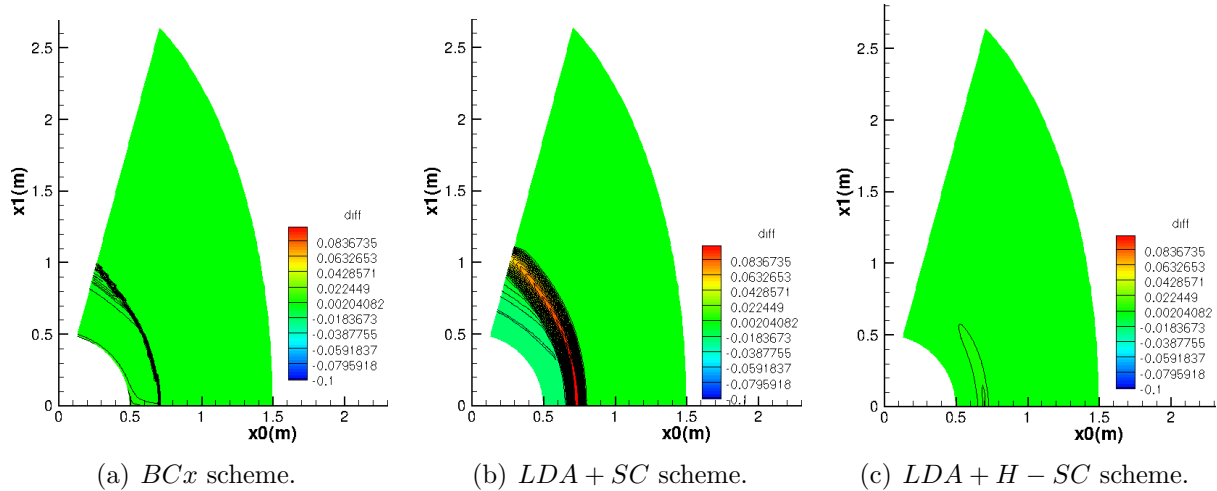
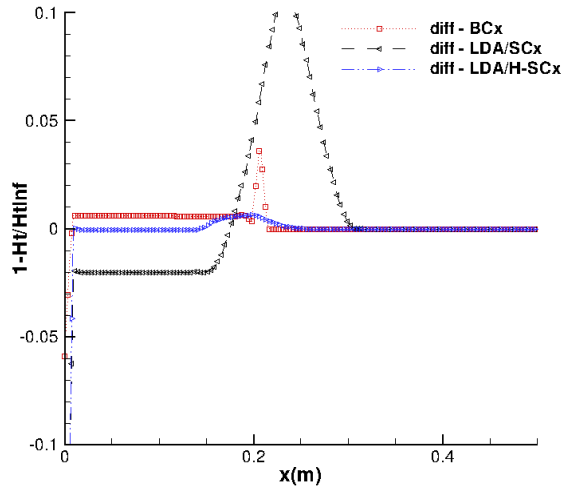
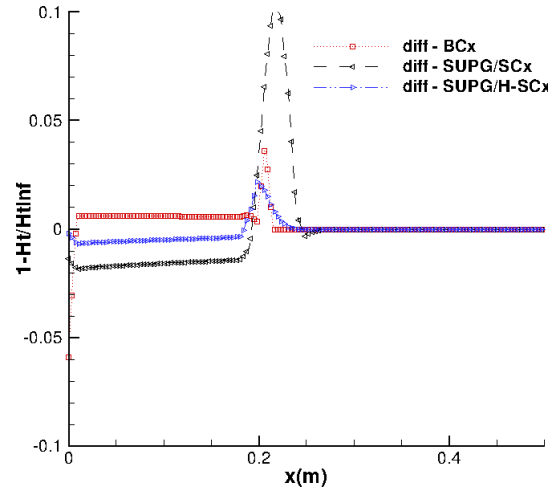


Figure 2: Inviscid, supersonic flow, $Ma_\infty = 9$. $\left(1 - \frac{H_t}{H_{t,\infty}}\right)$ -contours (50 levels in $[-0.1, 0.1]$)

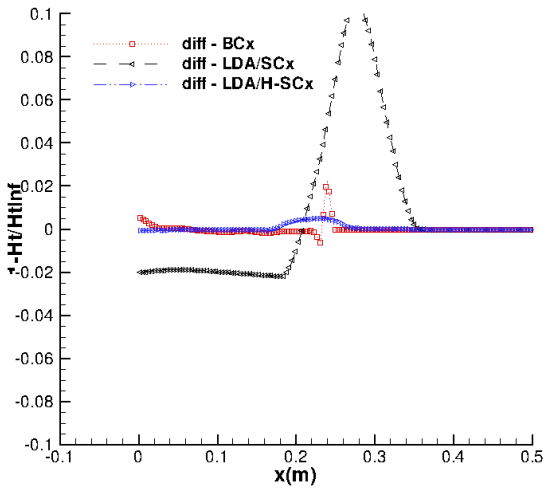


(a) *LDA + SC*

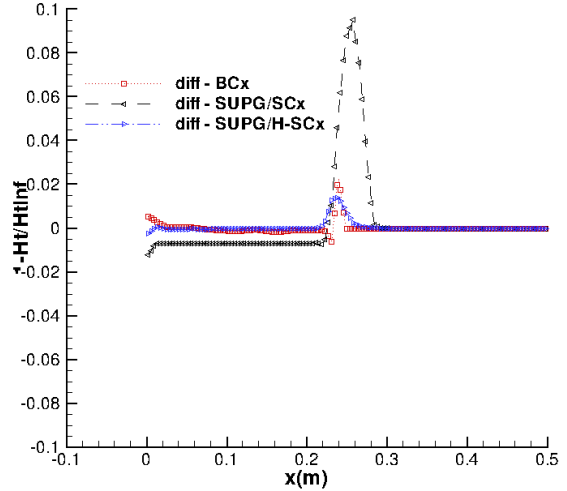


(b) *SUPG + SC*

Figure 3: Inviscid, hypersonic flow, $Ma_\infty = 9$. $\left(1 - \frac{H_t}{H_{t,\infty}}\right)$ along $y = 0$ m.



(a) *LDA + SC*



(b) *SUPG + SC*

Figure 4: Inviscid, hypersonic flow, $Ma_\infty = 9$. $\left(1 - \frac{H_t}{H_{t,\infty}}\right)$ along $y = 0.25$ m.

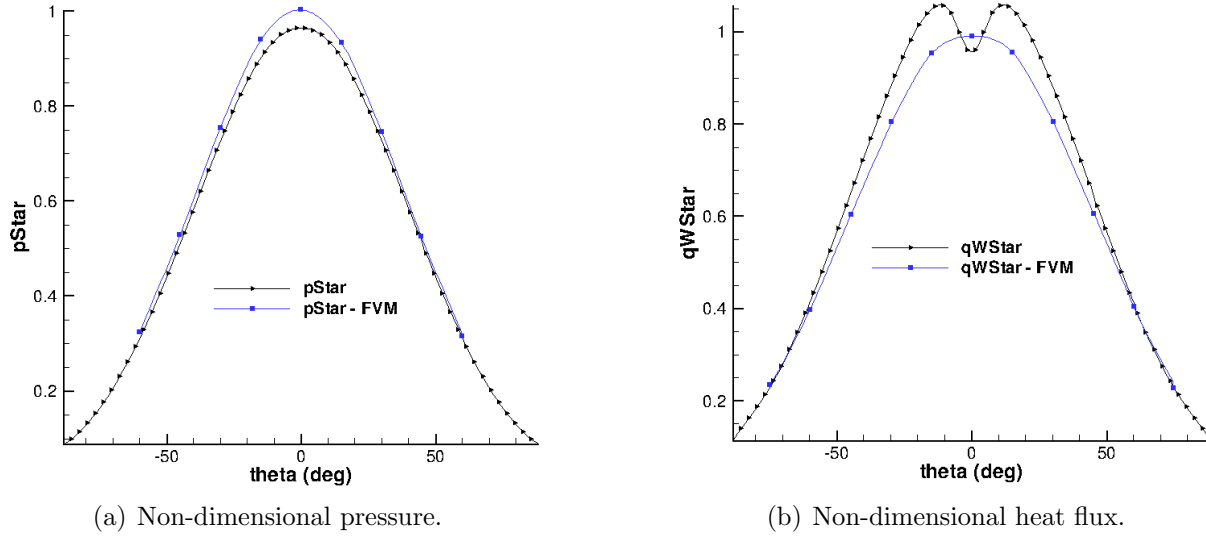


Figure 5: Viscous, hypersonic flow, $Ma_\infty = 8.1$. *LDA+H-SC* scheme. *FV* solution from reference¹⁴.

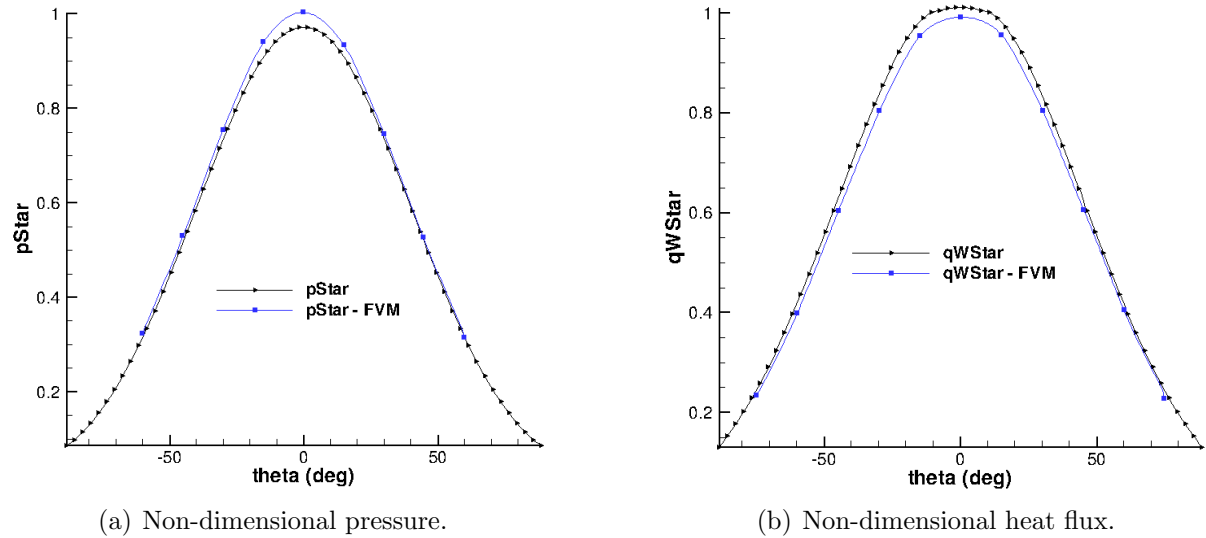


Figure 6: Viscous, hypersonic flow, $Ma_\infty = 8.1$. *SUPG+H-SC* scheme. *FV* solution from reference¹⁴.